Synthetic and Systems Biotechnology 10 (2025) 158–164

Contents lists available at ScienceDirect

Synthetic and Systems Biotechnology

journal homepage: www.keaipublishing.com/en/journals/synthetic-and-systems-biotechnology

Original Research Article

# Efficient biosynthesis of $\beta$-caryophyllene in *Saccharomyces cerevisiae* by $\beta$-caryophyllene synthase from *Artemisia argyi*

Zhengping Li [a], Yuhong Gan [a], Changyu Gou [a], Qiongyu Ye [a], Yang Wu [a], Yuhong Wu [a], Tingxing Yang [a], Baolian Fan [a], Aijia Ji [a], Qi Shen [b], Lixin Duan [a,*]

[a] *Guangdong Provincial Key Laboratory of Translational Cancer Research of Chinese Medicines, Joint International Research Laboratory of Translational Cancer Research of Chinese Medicines, International Institute for Translational Chinese Medicine, School of Pharmaceutical Sciences, Guangzhou University of Chinese Medicine, Guangzhou, 510006, PR China*

[b] *Institute of Medical Plant Physiology and Ecology, School of Pharmaceutical Sciences, Guangzhou University of Chinese Medicine, Guangzhou, 510006, PR China*

ARTICLE INFO

*Keywords:*
*Artemisia argyi*
$\beta$-caryophyllene
$\beta$-caryophyllene synthase
Biosynthesis
*Saccharomyces cerevisiae*

ABSTRACT

*Artemisia argyi* H. Lév. & Vaniot is an important traditional Chinese medicinal plant known for its volatile oils, which are the main active components of *A. argyi*, including monoterpenes, sesquiterpenes and their derivatives. Despite its medicinal significance, the biosynthesis of sesquiterpenoids in *A. argyi* remains underexplored. In this study, we identified four $\beta$-caryophyllene synthases from *A. argyi*. A high-yield $\beta$-caryophyllene engineered *Saccharomyces cerevisiae* cell factory has been built in this study. By fusing *ERG20* and *AarTPS88* with a flexible linker $(GGGS)_2$ and enhancing metabolic flux in the MVA pathway (*HIF-1*, *tHMGR*, and *UPC2-1*), we achieved a titer of $\beta$-caryophyllene reached 15.6 g/L by fed-batch fermentation in a 5 L bioreactor. To our knowledge, this represents the highest reported titer of $\beta$-caryophyllene in yeast to date. This study provides a valuable tool for the industrial-scale production of $\beta$-caryophyllene.

## 1. Introduction

*Artemisia argyi* H. Lév. & Vaniot, a perennial herb in the family Asteraceae, is used as a medical plant in folks for centuries [1,2]. *A. argyi* is abundant in volatile oils (mainly composed of monoterpenes, sesquiterpenes and their derivatives), flavonoids, and terpenoids, which possess pharmacological activities such as antioxidant, immunomodulatory, and anti-inflammatory effects [3,4]. Sesquiterpenoids, one of the key active components in *A. argyi*, are composed of three isoprene units and are synthesized by the action of sesquiterpene synthase using farnesyl pyrophosphate (FPP) as the substrate. Among these, $\beta$-caryophyllene, a bicyclic sesquiterpene, stands out due to its diverse physiological activities, such as anti-inflammatory and antioxidant properties [5,6]. It is also recognized by the FDA as a safe compound for use as a fragrance and flavoring agent. Additionally, $\beta$-caryophyllene is has garnered attention as a vital component in aviation fuels [7]. These sesquiterpenoids and other bioactive compounds from *A. argyi* are extensively utilized across pharmaceutical, food, and biofuel industries [8].

The content of terpenoids from plant sources is low and extraction is difficult. The synthetic biology of microorganisms is a promising way to produce terpenoids. Sesquiterpenes are mainly produced by plant extraction or chemical synthesis but are limited by long plant growth cycles, low content of sesquiterpenes and complex chemical structures [9]. In recent years, with the identification of more and more plant sesquiterpene synthases, it has become possible to biosynthesize many sesquiterpene compounds using microbial cells, such as artemisinic acid [10], $\beta$-elemene [11], and (−)-$\alpha$-bisabolol [12]. However, the synthesis pathway of $\beta$-caryophyllene has not been elucidated, and the key enzymes involved in its synthesis have not been identified in *A. argyi*.

Currently, metabolic engineering for $\beta$-caryophyllene production has been previously investigated in *E. coli* and yeasts (Table 1), but the yield is far from reaching the level that can be commercialized. In microorganisms, $\beta$-caryophyllene is produced by farnesyl pyrophosphate (FPP), an intermediate of the mevalonate pathway, catalyzed by $\beta$-caryophyllene synthase. Several metabolic engineering strategies have been established to enhance the production of terpene products in *S. cerevisiae* [13,14]. One common approach involves the fusion of

Peer review under responsibility of KeAi Communications Co., Ltd.
* Corresponding author.
*E-mail address:* nlizn@gzucm.edu.cn (L. Duan).

https://doi.org/10.1016/j.synbio.2024.09.005
Received 15 June 2024; Received in revised form 7 September 2024; Accepted 12 September 2024
Available online 22 September 2024

**Table 1**
Production of β-caryophyllene in engineered strains.

| Chassis | β-caryophyllene synthases | Shake flask Culture (mg/L) | Fed-batch fermentation (mg/L) | References |
|---|---|---|---|---|
| *S. cerevisiae* | AaQHS1$^{E353D}$ | 70.45 | 594.05 | [20] |
| *E. coli* | AaQHS1 | 220 | 1520 | [22] |
| *S. cerevisiae* | AaQHS1 | 250.4 | 2949.1 | [23] |
| *E. coli* | NtTPS7 | 100.3 | 5142 | [21] |
| *S. cerevisiae* | HbBaS | 206 | 8.47 g/L | [24] |
| *S. cerevisiae* | AarTPS88 | 828.4 | 15.6 g/L | This study |

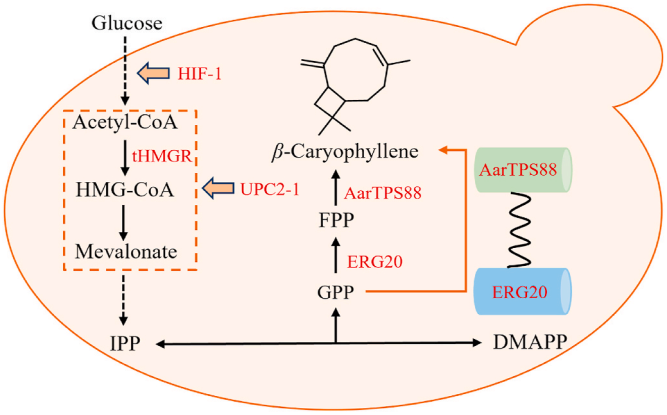


**Fig. 1.** Schematic diagram of heterologous biosynthesis of β-caryophyllene in *S. cerevisiae*. Overexpressed genes are presented in red. IPP, isopentenyl pyrophosphate; DMAPP, dimethylallyl pyrophosphate; GPP, geranyl diphosphate; tHMGR, truncated HMG-CoA reductase gene; ERG20, farnesyl diphosphate synthase; FPP, farnesyl diphosphate; HIF-1, hypoxia-inducible factor 1; UPC2-1, mutant of sterol uptake control protein 2; AarTPS88, β-caryophyllene synthase.

sesquiterpene synthase with FPP synthase (ERG20), which directs more FPP into the sesquiterpene synthesis pathway, thereby optimizing sesquiterpene synthesis [15]. Another crucial step in increasing precursor supply involves overexpressing the key rate-limiting enzyme tHMGR [16] and the transcription factor UPC2-1 [17]. In addition, "Warburg effect" is a metabolic trait that refers to the fact that most cancer cells rely on aerobic glycolysis for energy and tend to convert glucose to lactate even in the presence of aerobic support for mitochondrial oxidative phosphorylation [18]. Studies revealed that hypoxia-inducible factor-1 (HIF-1) complex (including *HIF-1α* and *ARNT*) could induce the Warburg effect in yeast to enhance glycolysis, thereby increasing acetyl-CoA flux, ultimately improving the production of downstream metabolites, and is a practical engineering strategy for the production of triterpenes in yeast [19]. Therefore, it is hypothesized that the optimization strategy of the complex was also applicable to the production of sesquiterpenes in yeast. Lu et al. heterologously produced β-caryophyllene in *Saccharomyces cerevisiae* at a titer of 594.05 mg/L [20]. The tobacco-derived β-caryophyllene synthase gene (*TPS7*) was overexpressed in *Escherichia coli* and optimized for the MVA pathway, with a final yield of 5142 mg/L [21].

In this study, four β-caryophyllene synthases (AarTPS88, AarTPS78, AarTPS54, and AarTPS61) were firstly cloned and characterized their biochemical functions from *A. argyi*. Based on the most catalytic efficient gene *AarTPS88,* we then constructed a *S. cerevisiae* cell factory with the titer of β-caryophyllene reaching 15.6 g/L in a 5 L bioreactor, which is the highest titer reported so far in yeast ( Fig. 1). This study presents a valuable tool for the industrial-scale production of β-caryophyllene, also provides strategies to be used in increasing other terpenoid production and strain constructions.

## 2. Materials and methods

### 2.1. Plant materials

*A. argyi* was taken in the greenhouse of Guangzhou University of Chinese Medicine in July 2023. The plants were frozen in liquid nitrogen and stored at −80 °C for later use.

### 2.2. Bioinformatic analysis

Through analyzing the transcriptome data of *A. argyi* sequenced by Qi Shen's group at the Institute of Medicinal Plant Physiology and Ecology, School of Chinese Medicine, Guangzhou University of Chinese Medicine. The candidate terpene synthases genes were potentially screened out from the transcriptome data by the local blast method using the known sesquiterpene synthase protein sequences. Four candidate *AarTPSs* genes were then aligned and constructed a neighbor-joining (NJ) phylogenetic tree with characterized terpene synthase genes [25] (https://www.bioinformatics.nl/sesquiterpene/synthasedb/, Table S3) using the ClustalW program of MEGA11. Phylogenetic analysis was conducted using the neighbor-joining method (1000 bootstrap replicates). The resulting phylogenetic trees were beautified using the ChiPlot website (ChiPlot). Additionally, the conserved regions were presented by the BioEdit software.

### 2.3. Quantitative real-time PCR

Total RNA was extracted from the roots, stems, and leaves of *A. argyi* using the Quick RNA Isolation Kit (Huayueyang, Beijing). Reverse transcription was carried out with the *Evo M-MLV* RT Kit with gDNA Clean for qPCR II (Accurate Biotechnology (Hunan) Co., Ltd.). qRT-PCR was performed following the instructions provided with the SYBR® Green Premix *Pro Taq* HS qPCR Kit, and primers were designed using Primer Premier 6 software (Table S4). *Actin* was selected as a reference gene [26]. The relative gene expression levels were determined using the $2^{-\Delta\Delta CT}$ method [27].

### 2.4. Cloning of AarTPSs and construction of yeast strains

Total RNA was extracted from roots, stems, and leaves of *A. argyi* using the Quick RNA Isolation Kit (Huayueyang Biotechnology Co., Ltd., Beijing, China, Product No. 0416-50). The total RNA was reverse transcribed into first-strand cDNA strand using *Evo M-MLV* Plus 1st Strand cDNA Synthesis Kit, following the manufacturer's protocol. The candidate *AarTPSs* genes were amplified from the *A. argyi* cDNA using high-fidelity DNA polymerase (Novagen) and gene-specific primers (Table S1). The amplified fragments were cloned into the *BamHI* and *NheI* sites of yeast expression vector pESC-URA using the ClonExpress II One Step Cloning Kit (Vazyme Biotech Co., Ltd) and verified by sequencing (Sangon Biotech (Shanghai) Co., Ltd.).

The constructed expression plasmids pESC-Ura-*AarTPSs* were heterologously expressed in the yeast strain SE00 (yYF601 with the *GAL80* gene knocked out) via the LiAc/SS carrier DNA/PEG method [28]. A fusion expression vector ERG20-$(GGGS)_2$-AarTPS88 was built according to the literature [12]. ERG20 was fused with AarTPS88 by linker $(GGGS)_2$, and the fusion fragment was into the *BamHI* and *NheI* sites of yeast expression vector pESC-URA. The transformed cells were then spread on plates of synthetic complete medium lacking uracil, incubated at 30 °C for 2–3 days and positively screened for single colonies by PCR. The plasmids and strains used in this study, as well as the amino acid sequences of the four AarTPSs are shown in Tables S2 and S5, respectively.

### 2.5. Shake flask culture and bioreactor fermentation

Yeast strains were cultured in YPD medium (10 g/L yeast extract, 20

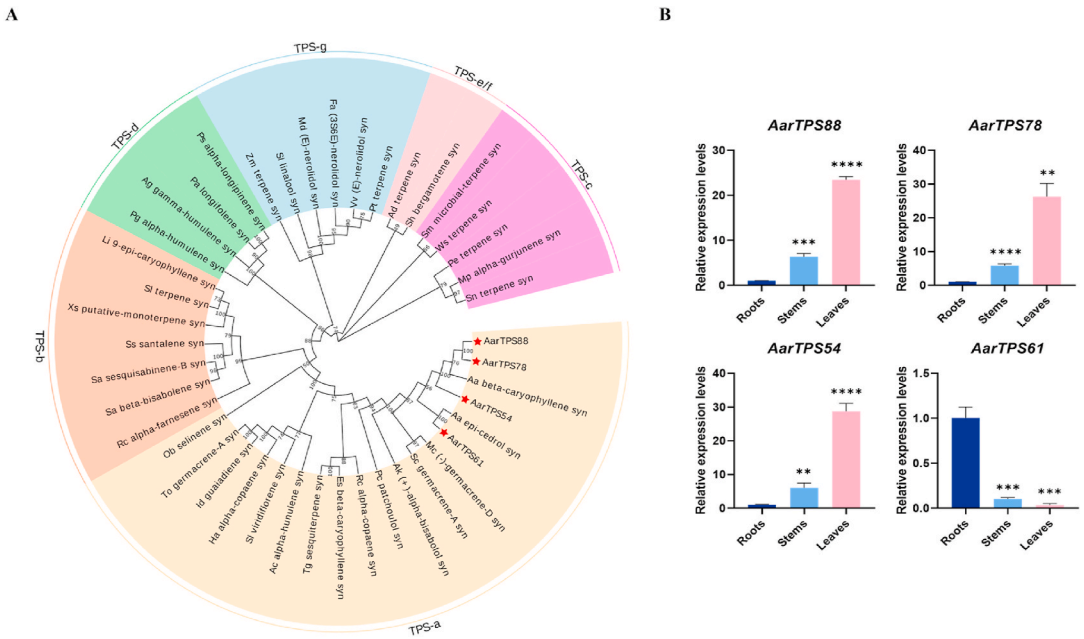


**Fig. 2.** Analysis of the four candidate genes from *A. argyi*. A. Phylogenetic analysis of AarTPSs. The TPS family divided into six subfamilies, the TPS-a family to the TPS-e/f family, these are denoted by unusual colors. B. qRT-PCR expression analysis of *AarTPSs* in different tissues. The error bars represent the means ± SD (n = 3), $^{**}P < 0.01$, $^{***}P < 0.001$, and $^{****}P < 0.0001$ in Student's t-test.

g/L peptone and 20 g/L glucose) or SD Medium (6.7 g/L yeast nitrogen base, 1.3 g/L of amino acid drop-out mix, 20 g/L glucose). Single-colonies were selected from the plates and incubated in a shaking tube with 3 mL culture medium for 12 h. The culture was then transferred to a 250 mL shake flask containing 50 mL medium at an inoculum volume 1 %. The culture conditions maintained at 30 °C, 200 rpm for 5 days. After 12 h of incubation, 10 % n-dodecane was added to capture the product, which was subsequently used for subsequent qualitative or quantitative analysis. All cultivations were performed in triplicate.

Bioreactor fermentation was conducted in a 5 L bioreactor (BIOTECH, Bxbio, China).The fermentation medium was contained 15 g/L $(NH_4)_2SO_4$, 8 g/L $KH_2PO_4$, 6.14 g/L $MgSO_4•7H_2O$, 0.72 g/L $ZnSO_4•7H_2O$, 20 g/L glucose, 10 mL/L trace metals (2.8 g/L $FeSO_4•7H_2O$, 5.75 g/L $ZnSO_4•7H_2O$, 2.9 g/L $CaCl_2•2H_2O$, 0.32 g/L $MnCl_2•4H_2O$, 0.47 g/L $CoCl_2•6H_2O$, 0.32 g/L $CuSO_4$, 0.48 g/L $Na_2MoO_4•2H_2O$, 80 mg/L 0.5 M EDTA) and 12 mL/L vitamin solution (50 mg/L biotin, 1.0 g/L calcium pantothenate, 1.0 g/L thiamine hydrochloride, 1.0 g/L pyridoxal hydrochloride, 1.0 g/L nicotinic acid, 0.2 g/L p-aminobenzoic acid, 25 g/L inositol). The single colony seeds were picked and inoculated into a tube containing 5 mL YPD medium, cultured at 30 °C, 200 rpm for 36 h. This culture was then transferred into a 100 mL shake flask containing 20 mL YPD medium for 24 h at 30 °C and 200 rpm. Subsequently, the second seed culture was transferred into a 500 mL shake flask containing 200 mL YPD medium for 24 h at 200 rpm and 30 °C. Finally, the seeds were inoculated into the bioreactor filled with 1.8 L medium. Fermentation was carried out at 30 °C, with the pH adjusted at 5.5 using ammonia hydroxide. The agitation cascade (300–900 rpm) was coupled with dissolved oxygen saturation at 40 %, and the airflow rate was 1 vvm. Ethanol was fed as the carbon source. After fermenting for 120 h, the yield of *β*-caryophyllene was analyzed by GC-MS.

### 2.6. GC-MS analytical methods

The GC-MS analysis was performed on a Shimadzu QP2010SE instrument equipped with a Rxi-5HT column (30 m × 250 μm × 0.25 μm). The heating program was as follows: the initial temperature was 40 °C for 3 min, then raised to 130 °C at 10 °C/min, followed by an increase to 160 °C at 3 °C/min, and finally to 250 °C at 40 °C/min. The electron energy was set at 70 eV, with the ion source and interface temperature at 250 °C and 170 °C, respectively. The scanning range was 50–600 *m/z*. All products in this study were identified by comparison with the National Institute of Standards and Technology (NIST)17 mass spectral library and authentic standards. *α*-Caryophyllene (CAS: 6753-98-6) and *β*-caryophyllene (CAS: 87-44-5) standards were purchased from Macklin.

## 3. Results and discussion

### 3.1. Phylogenetic and qRT-PCR analysis of TPSs from A. argyi

The full-length sequences of the four candidate genes, ranging from 1635 to 1650 bp and encoding 545–550 amino acids, were obtained by PCR amplification using *A. argyi* cDNA as template. Phylogenetic analysis (Fig. 2A) showed that the four AarTPSs belonged to the TPS-a subfamily, AarTPS88, AarTPS78, AarTPS54, and AarTPS61 were closely related to *β*-caryophyllene synthase from *Artemisia annua* [29]. In contrast, AarTPS61 showed higher similarity to epi-cedrol synthase from *Artemisia annua* [30]. Like all characterized plant terpene synthases, the four AarTPSs contain several motifs that are highly conserved among class I terpene synthases, such as the C-terminal structural domain containing two metal-binding motifs of aspartate-rich DDXXD and NSE/DTE, and the N-terminal $RRX_8W$ motif (Fig. S1) [31–33]. This motifs are critical for catalytic activity of terpene synthases and play essential roles in sesquiterpene synthases [34]. Therefore, we hypothesized that the four AarTPSs may have similar functions to the *β*-caryophyllene and epi-cedrol synthases.

Furthermore, we extracted the RNA sample from the roots, stems and leaves of *A. argyi,* analyzed the expression levels of the four AarTPS candidate genes using qRT-PCR. The results (Fig. 2B) showed that *AarTPS61* was highly expressed in roots, and lowly expressed in leaves and stems. The expression of the other three genes showed a similar trend, all of which were significantly highly expressed in leaves and almost not expressed in roots. Similar expression levels of four *AarTPSs* existed in qRT-PCR and transcriptome (Fig. S2).

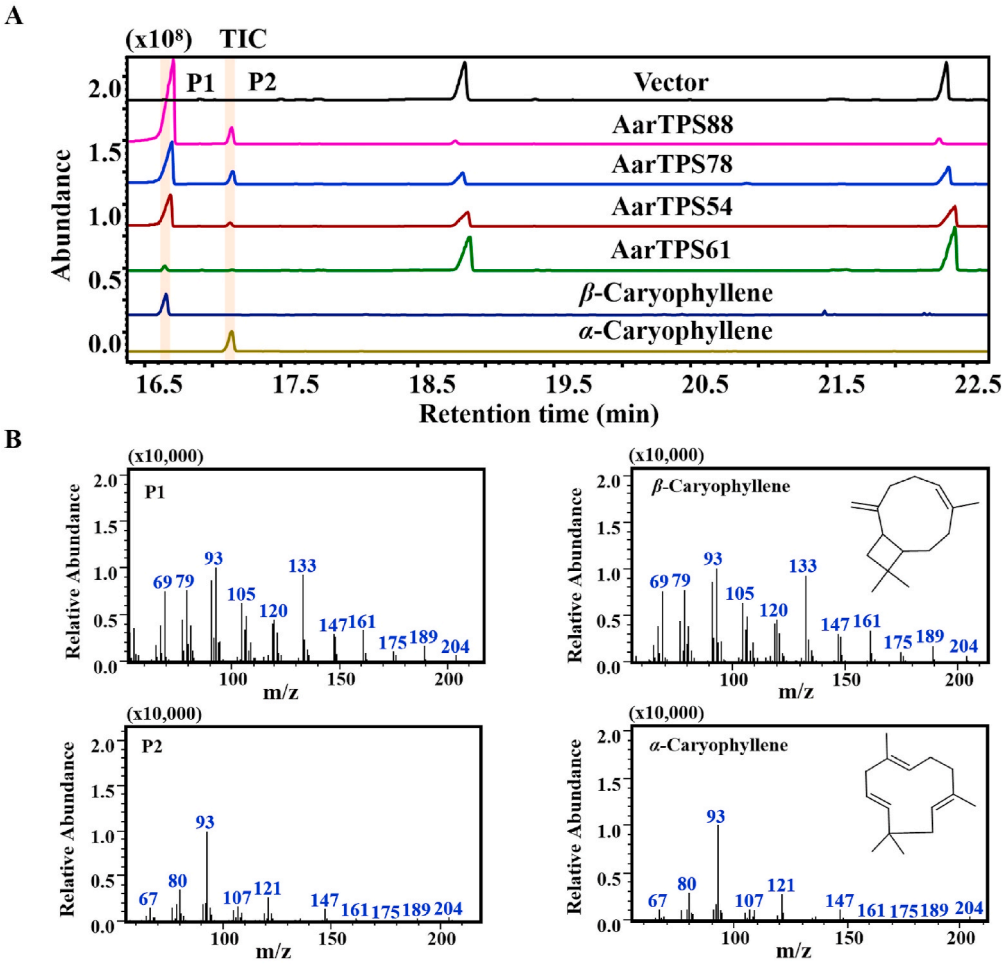


**Fig. 3.** The products analyzed and identified by GC-MS. A. Total ion gas chromatogram of AarTPS88, AarTPS78, AarTPS54, and AarTPS61. B. Mass spectra of the product P1, P2 and standards.

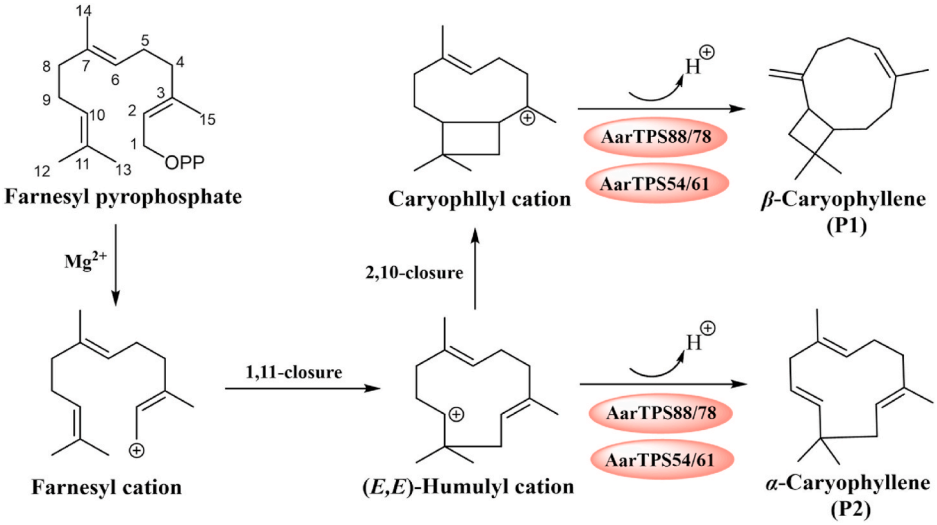


**Fig. 4.** Proposed $\alpha$-caryophyllene and $\beta$-caryophyllene biosynthetic pathways in *A. argyi*.

### 3.2. Functional characterization of AarTPSs in S. cerevisiae

The four *AarTPSs* genes were transformed into the heterologous host yeast strain SE00. The TIC plots of these transformations were compared with the empty vector to identify the catalytic products of *AarTPSs*. As shown in Fig. 3A and B, AarTPS88, AarTPS54, AarTPS78, and AarTPS61 had a major product (P1) at 16.66 min. P1 was identified as $\beta$-caryophyllene by comparing the retention time and mass spectra with the $\beta$-caryophyllene standard. The retention time of the minor product (P2) at 17.09 min was identified as $\alpha$-caryophyllene with the standard.

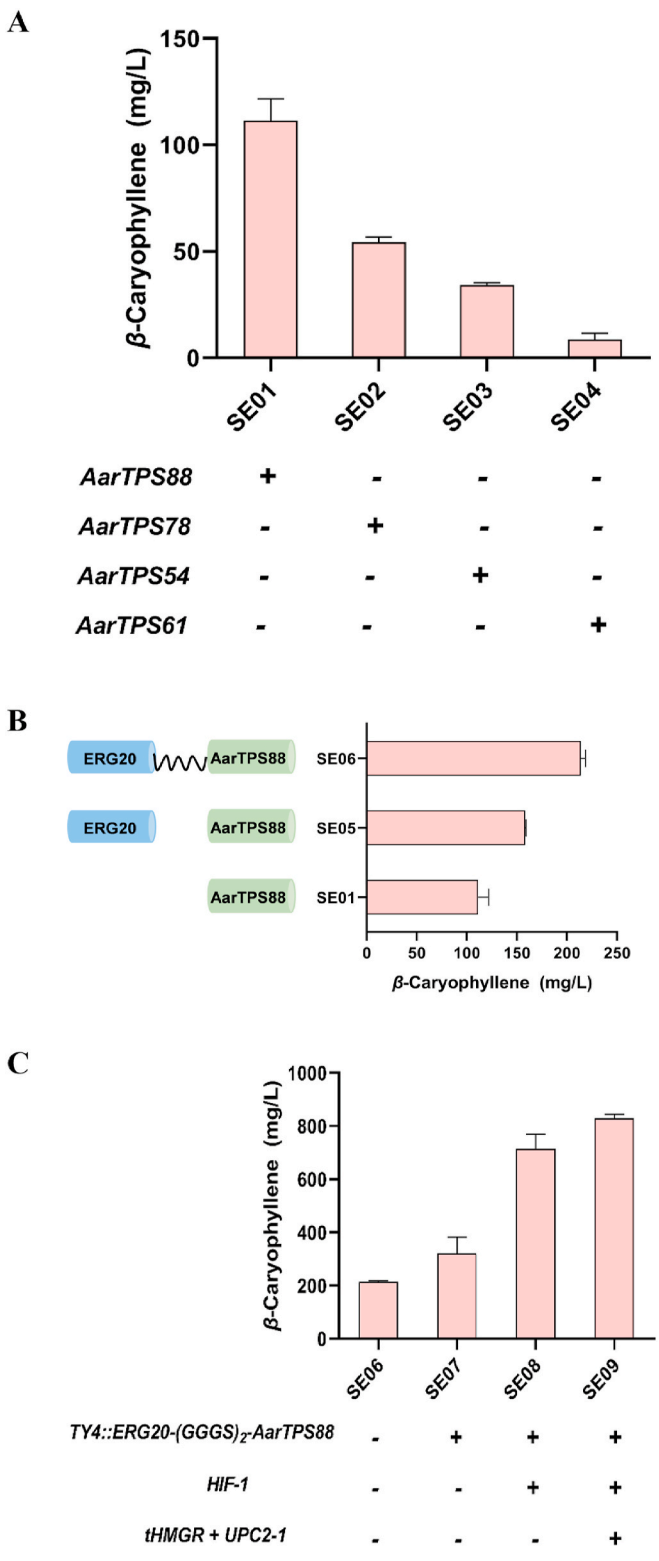


**Fig. 5.** Construction of recombinant *S. cerevisiae* strains to produce β-caryophyllene. A. β-Caryophyllene yield of strains SE01, SE02, SE03, and SE04. B. Improving β-caryophyllene production by fusion expression of AarTPS88 and ERG20. C. β-Caryophyllene production by overexpression of a fusion expression cassette of ERG20 and AarTPS88 and genes such as *HIF1*, *tHMGR* and *UPC2-1*. Error bars represent the SD of triplicate samples.

Therefore, these four genes encode the β-caryophyllene synthase, producing β-caryophyllene, consistent with their similarity to β-caryophyllene synthase in phylogenetic analysis (Fig. 2A). Thus, we identified four β-caryophyllene synthase genes from *A. argyi* (see Fig. 4).

### 3.3. Fusion expression of ERG20 and AarTPS88 to enhance β-caryophyllene production

To construct an engineered strain for the efficient biosynthesis of β-caryophyllene in *S. cerevisiae*, we transformed plasmids into strain SE00, resulting in strains SE01-04 (Table S2). Among these, strain SE01 produced the highest rield of β-caryophyllene at 111.3 mg/L (Fig. 5A). Although this yield was relatively low, it indicates that the yield of β-caryophyllene can be further improved by optimizing the biosynthetic pathway.

Protein fusion technology can shorten the distance between two enzymes, increase the utilization rate of intermediate metabolites, and thereby improve the catalytic efficiency of the entire pathway, making it a crucial strategy in metabolic engineering [35]. It has been observed that different flexible linkers affect the catalytic activity of enzymes to varying degrees, with the most suitable flexible linker identified as $(GGGS)_2$ [9,36]. FPP originating from the MVA pathway, is catalyzed by FPP synthase (ERG20) and serves as a direct precursor for the synthesis of β-caryophyllene. Therefore, we expressed ERG20 and AarTPS88 individually to obtain strain SE05, and fused ERG20 with AarTPS88 using flexible linker $(GGGS)_2$ to obtain strain SE06 (Fig. 5B). The most significant increase in β-caryophyllene production was observed in strain SE06 at 213.9 mg/L, which was 92 % higher compared to strain SE01. These results indicate that the biosynthesis of β-caryophyllene benefits from enzyme fusion expression. Based on this, we integrated the ERG20 and AarTPS88 fusion expression cassette into the chromosome of strain SE00 for overexpression, generating strain SE07. The β-Caryophyllene titer in strain SE07 reached 320.6 mg/L, which was 49 % higher than that of strain SE06 (Fig. 5C).

### 3.4. Engineering the MVA synthesis pathway to further improve β-caryophyllene biosynthesis

To trigger the Warburg effect in yeast, which is similar to aerobic glycolysis in cancer cells. We integrated *HIF-1* into the yeast chromosome of strain SE07 to derive strain SE08. The results showed that the titer of β-caryophyllene in the shake flask reached 713.6 mg/L, which increased the yield by 2.2 times (Fig. 5C). This indicates that the hypoxia-inducible factor-1 (*HIF-1)* is also suitable for increasing the production of sesquiterpenes in yeast.

In yeast, the FPP of the MVA pathway is the direct precursor for sesquiterpenes synthesis, and the limited supply of precursor is the

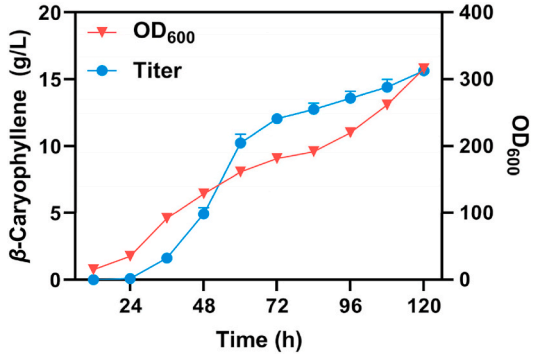


**Fig. 6.** Efficient production of β-caryophyllene by fed-batch fermentation of strain SE09. Fed-batch fermentation was performed in a 5 L bioreactor. Titer of β-caryophyllene and biomass ($OD_{600}$) are monitored during fermentation. The data shown are calculated from three biological replicates.

major limitation and one of the focal points of microbial sesquiterpene synthesis. Therefore, overexpression of the key gene *tHMGR* in the MVA pathway can increase the biosynthesis of sesquiterpenes [37]. Additionally, *UPC2-1*, a single mutant (G888D) of the *UPC2* transcriptional activator of the MVA pathway, similarly increases terpene synthesis [38]. Therefore, the expression vector containing *tHMGR* and *UPC2-1* was transformed into the chromosome of strain SE08, generating strain SE09. GC-MS analysis showed that the $\beta$-caryophyllene yield of strain SE09 was 828.4 mg/L, a 16 % increase (Fig. 5C). This indicates that the optimization of *tHMGR* and *UPC2-1* was effective. A similar optimization strategy (*tHMGR* and *UPC2-1* overexpression) has also been reported for squalene production in *S. cerevisiae* [39].

### 3.5. Fed-batch fermentation to produce high-level $\beta$-caryophyllene

Finally, we evaluated the performance of the engineered strain SE09 as a $\beta$-caryophyllene cell factory using fed-batch fermentation in a 5 L bioreactor. To capture the product, 10 % n-dodecane was added at 12 h. As shown in Fig. 6, the growth of engineered strain SE09 was slight inhibited during the 24 h, but exhibited rapidly growth in the later stages. The cell density ($OD_{600}$) reached 315 at 120 h, with the $\beta$-caryophyllene titer reaching 15.6 g/L, representing the highest reported $\beta$-caryophyllene titer in yeast to date.

Although $\beta$-caryophyllene production in *S. cerevisiae* has been significantly enhanced through metabolic pathway optimization and fed-batch fermentation, further improvements can be achieved in subsequent studies. Potential strategies include altering the catalytic activity of sesquiterpene synthases through site-directed mutagenesis [38]; inhibition of the competitive pathway by knockdown of the lipid phosphatase LPP1 and diacylglycerol pyrophosphate phosphatase DPP1 [40]; and promoting extracellular secretion of sesquiterpenes by enhancing transmembrane transport to enhance $\beta$-caryophyllene production [13].

## 4. Conclusions

In summary, this study functionally characterized four *AarTPS* candidate genes from *A. argyi* in *S. cerevisiae,* identifying them as $\beta$-caryophyllene synthase. Next, we constructed an engineered strain with a high titer of $\beta$-caryophyllene by using fusion expression and heterologous gene expression to increase MVA pathway flux. The engineered strain achieved a $\beta$-caryophyllene titer of 15.6 g/L in a 5 L bioreactor, laying the foundation for developing an *S. cerevisiae* cell factory for industrial scale $\beta$-caryophyllene production.

## Funding

This research was supported by the National Natural Science Foundation of China No.81874333.

## CRediT authorship contribution statement

**Zhengping Li:** Writing – original draft, Methodology, Data curation. **Yuhong Gan:** Software, Methodology, Data curation. **Changyu Gou:** Methodology, Data curation. **Qiongyu Ye:** Software, Data curation. **Yang Wu:** Methodology, Data curation. **Yuhong Wu:** Methodology, Data curation. **Tingxing Yang:** Methodology, Data curation. **Baolian Fan:** Writing – original draft, Methodology. **Aijia Ji:** Supervision, Software. **Qi Shen:** Supervision, Resources. **Lixin Duan:** Writing – review & editing, Supervision, Project administration, Methodology, Funding acquisition, Conceptualization.

## Declaration of competing interest

The authors declare that they have no known competing financial interests or personal relationships that could have appeared to influence the work reported in this paper.

## Acknowledgements

We are grateful to Prof. Xiaozhou Luo from Shenzhen Institutes of Advanced Technology, Chinese Academy of Sciences, for providing the yeast strain yYF601 and Prof. Tianyue An from School of Integrated Traditional Chinese and Western Medicine, Binzhou Medical University, for providing the plasmid pTP-URA–HIF–1α-ARNT.

## Appendix A. Supplementary data

Supplementary data to this article can be found online at https://doi.org/10.1016/j.synbio.2024.09.005.

## References

[1] Chizzola R, Gansinger D. Chemical composition and antioxidant activity of *Artemisia argyi* essential oil and hydrolate. Compounds 2023;3(3):521–31.
[2] Song X, Wen X, He J, et al. Phytochemical components and biological activities of *Artemisia argyi*. J Funct Foods 2019;52:648–62.
[3] Chen H, Guo M, Dong S, et al. A chromosome-scale genome assembly of *Artemisia argyi* reveals unbiased subgenome evolution and key contributions of gene duplication to volatile terpenoid diversity. Plant Commun 2023;4(3):100516–31.
[4] Miao Y, Luo D, Zhao T, et al. Genome sequencing reveals chromosome fusion and extensive expansion of genes related to secondary metabolism in *Artemisia argyi*. Plant Biotechnol J 2022;20(10):1902–15.
[5] Liang B, Yang Q, Zhang X, et al. Switching carbon metabolic flux for enhancing the production of sesquiterpene-based high-density biofuel precursor in *Saccharomyces cerevisiae*. Biotechnol Biofuels Bioprod 2023;16(1):124–36.
[6] Yang J, Nie Q. Engineering *Escherichia coli* to convert acetic acid to $\beta$-caryophyllene. Microb Cell Fact 2016;15:74–82.
[7] Wu W, Liu F, Davis RW. Engineering *Escherichia coli* for the production of terpene mixture enriched in caryophyllene and caryophyllene alcohol as potential aviation fuel compounds. Metab Eng Commun 2018;6:13–21.
[8] Belcher MS, Mahinthakumar J, Keasling JD. New frontiers: harnessing pivotal advances in microbial engineering for the biosynthesis of plant-derived terpenoids. Curr Opin Biotechnol 2020;65:88–93.
[9] Luo Y, Li BZ, Liu D, et al. Engineered biosynthesis of natural products in heterologous hosts. Chem Soc Rev 2015;44(15):5265–90.
[10] Li C, Li J, Wang G, et al. Heterologous biosynthesis of artemisinic acid in *Saccharomyces cerevisiae*. J Appl Microbiol 2016;120(6):1466–78.
[11] Liu Q, Zhang G, Su L, et al. Reprogramming the metabolism of oleaginous yeast for sustainably biosynthesizing the anticarcinogen precursor germacrene A. Green Chem 2023;25(20):7988–97.
[12] Jiang Y, Xia L, Gao S, et al. Engineering *Saccharomyces cerevisiae* for enhanced (-)-$\alpha$-bisabolol production. Synth Syst Biotechnol 2023;8(2):187–95.
[13] Paramasivan K, Mutturi S. Progress in terpene synthesis strategies through engineering of *Saccharomyces cerevisiae*. Crit Rev Biotechnol 2017;37(8):974–89.
[14] Vickers CE, Williams TC, Peng B, et al. Recent advances in synthetic biology for engineering isoprenoid production in yeast. Curr Opin Chem Biol 2017;40:47–56.
[15] Mai J, Li W, Ledesma-Amaro R, et al. Engineering plant sesquiterpene synthesis into yeasts: a review. J Agric Food Chem 2021;69(33):9498–510.
[16] Polakowski T, Stahl U, Lang C. Overexpression of a cytosolic hydroxymethylglutaryl-CoA reductase leads to squalene accumulation in yeast. Appl Microbiol Biotechnol 1998;49(1):66–71.
[17] Ro DK, Paradise EM, Ouellet M, et al. Production of the antimalarial drug precursor artemisinic acid in engineered yeast. Nature 2006;440(7086):940–3.
[18] Vander Heiden MG, Cantley LC, Thompson CB. Understanding the Warburg effect: the metabolic requirements of cell proliferation. Science 2009;324(5930):1029–33.
[19] Lin X, An T, Fu D, et al. Optimization of central carbon metabolism by Warburg effect of human cancer cell improves triterpenes biosynthesis in yeast. Adv Biotechnol 2023;1:4–14.
[20] Lu S, Deng H, Zhou C, et al. Enhancement of $\beta$-caryophyllene biosynthesis in *Saccharomyces cerevisiae* via synergistic evolution of $\beta$-caryophyllene synthase and engineering the chassis. ACS Synth Biol 2023;12(6):1696–707.
[21] Cheng T, Zhang K, Guo J, et al. Highly efficient biosynthesis of $\beta$-caryophyllene with a new sesquiterpene synthase from tobacco. Biotechnol Biofuels Bioprod 2022;15(1):39–52.
[22] Yang J, Li Z, Guo L, et al. Biosynthesis of $\beta$-caryophyllene, a novel terpene-based high-density biofuel precursor, using engineered *Escherichia coli*. Renew Ener 2016;99:216–23.
[23] Li XD, Yang CS, Wang PP, et al. Production of sesquiterpenoids $\alpha$-neoclovene and $\beta$-caryophyllene by engineered *Saccharomyces cerevisiae*. Syn Bio J 2021;2(5):792–803.
[24] Shi B, Lou J, Yang ZR, et al. Construction of engineering *Saccharomyces cerevisiae* with a new $\beta$-caryophyllene synthase from *Hevea brasiliensis*. China Brew 2023;42(8):147–52.
[25] Durairaj J, Girolamo AD, Bouwmeester HJ, et al. An analysis of characterized plant sesquiterpene synthases. Phytochemistry 2019;158:157–65.

[26] Yi XZ, Wu L, Xiang L, et al. Screening of reference genes for quantitative real-time PCR in *Artemisia argyi*. China J Chin Mater Med 2022;47(3):659–67.
[27] Livak K.J., Schmittgen T.D. Analysis of relative gene expression data using real-time quantitative PCR and the $2^{-\Delta\Delta CT}$ method. Methods 25(4):402–408.
[28] Gietz RD, Schiestl RH. High-efficiency yeast transformation using the LiAc/SS carrier DNA/PEG method. Nat Protoc 2007;2(1):31–4.
[29] Cai Y, Jia JW, Crock J, et al. A cDNA clone for $\beta$-caryophyllene synthase from *Artemisia annua*. Phytochemistry 2002;61(5):523–9.
[30] Mercke P, Crock J, Croteau R, et al. Cloning, expression, and characterization of epi-cedrol synthase, a sesquiterpene cyclase from *Artemisia annua* L. Arch Biochem Biophys 1999;369(2):213–22.
[31] Kiran NR, Narayanan AK, Mohapatra S, et al. Analysis of root volatiles and functional characterization of a root-specific germacrene A synthase in *Artemisia pallens*. Planta 2024;259(3):58–70.
[32] Gao K, Lin Y, Li L, et al. Characterization of SchTPSs enables construction of yeast for the bioproduction of $\alpha$-cadinol and the related sesquiterpenes. J Agric Food Chem 2023;71(47):18424–30.
[33] Zhang J, Wang X, Zhang X, et al. Sesquiterpene synthase engineering and targeted engineering of $\alpha$-santalene overproduction in *Escherichia coli*. J Agric Food Chem 2022;70(17):5377–85.
[34] Ran J, Li Y, Wen X, et al. Identification of sesquiterpene synthase genes in the genome of *Aquilaria sinensis* and characterization of an $\alpha$-humulene synthase. J Res 2022;34(4):1117–31.
[35] Dai Z, Liu Y, Huang L, et al. Production of miltiradiene by metabolically engineered *Saccharomyces cerevisiae*. Biotechnol Bioeng 2012;109(11):2845–53.
[36] Ma B, Liu M, Li ZH, et al. Significantly enhanced production of patchoulol in metabolically engineered *Saccharomyces cerevisiae*. J Agric Food Chem 2019;67 (31):8590–8.
[37] Fordjour E, Liu CL, Hao Y, et al. Engineering *Escherichia coli* BL21 (DE3) for high-yield production of germacrene A, a precursor of $\beta$-elemene via combinatorial metabolic engineering strategies. Biotechnol Bioeng 2023;120(10):3039–56.
[38] Zhang W, Guo J, Wang Z, et al. Improved production of germacrene A, a direct precursor of $\beta$-elemene, in engineered *Saccharomyces cerevisiae* by expressing a cyanobacterial germacrene A synthase. Microb Cell Fact 2021;20(1):7–21.
[39] Zha W, An T, Li T, et al. Reconstruction of the biosynthetic pathway of santalols under control of the GAL regulatory system in yeast. ACS Synth Biol 2020;9(2): 449–56.
[40] Scalcinati G, Knuf C, Partow S, et al. Dynamic control of gene expression in Saccharomyces cerevisiae engineered for the production of plant sesquitepene $\alpha$-santalene in a fed-batch mode. Metab Eng 2012;14(2):91–103.